Type	γ_1	γ_2	γ_3	κ_1	κ_2	κ_3
A ($\gamma_2, \gamma_3 \gg \gamma_1$)	0.1	2	3	0.25	0.2	1
B ($\gamma_2 \gg \gamma_1, \gamma_3$)	0.1	10	0.25	1	0.5	1
C ($\gamma_1 > \gamma_2 + \gamma_3$)	1	0.1	0.25	1	0.1	1

Table 5.1: Parameter sets for Maxwell-Bloch equation.

5.5.2 Nonlinear Dynamics in Laser: Maxwell-Bloch equation

A semiclassical model of the laser is known as Maxwell-Bloch equation[5, 6]:

$$\dot{E} = -\gamma_1 E + \kappa_1 P \tag{5.39a}$$

$$\dot{P} = -\gamma_2 P + \kappa_2 E\, D \tag{5.39b}$$

$$\dot{D} = -\gamma_3 (D - \lambda) - \kappa_3 E\, P \tag{5.39c}$$

where E, P, D are the electric field, the mean polarization of atoms, and the population inversion, respectively. γ_1 are the decay rates of the electric field in the laser cavity due to beam transmission. γ_2 and γ_3 are the decay rates of the atomic polarization and population inversion, respectively. $\kappa_i, i = 1, 2, 3$ are positive coupling constants. λ is the energy pumping parameter and may be positive, negative or zero. Unlike two-dimensional nonlinear dynamics of the Brusselator model, this is three-dimensional nonlinear dynamics and chaotic trajectories are possible. Depending on the parameter values, the system shows a variety of dynamics. We solve the coupled ODEs using 2nd-order Runge-Kutta method from $t = 0$ to $t = 500$ (or longer) for each parameter set given in Table 5.1. Then, we investigate the time evolution of E and two-dimensional phase trajectory (E, D) for each of the following cases. Type C shows a particularly interesting trajectory known as *strange atractor* which is confined in a finite region without repeating itself as shown in Fig. 5.11. Such a trajectory is possible only in three or higher dimensional phase spaces.

Type A Vary λ from 3.0 to 6.0. Observe that E always converges to a constant value. However, below a certain critical value of λ, E decays to zero. On the other hand, above it E goes to a positive vale (lasing).

Type B Vary λ from 0.5 to 3. Observe that E always converges to a constant value. However, below a certain critical value of λ, E decays to zero. On the other hand, above it E goes to a positive vale (lasing).

Type C Vary λ from 20 to 25. Observe that E decays to zero with oscillation below a critical value of λ. Above the critical value, E randomly oscillates (unstable laser).

5.5.3 Frequency Entrainment and Phase Synchronization

Rhythmical oscillations are ubiquitous phenomena such as heart beat, burst of neuron, circadian rhythm and hands clapping. Each oscillation has its own frequency, phase, and amplitude. Consider a large number of oscillators interacting each other. Each oscillator has a slightly different frequency and phase from each others. With an appropriate interaction, the all oscillators begin oscillating in unison with the identical frequency and the same phase despite that individual oscillators have different natural frequencies. This is the phenomenon of synchronization.[7] For example imagine hand clapping at the end of a ballet performance. At the beginning, the clapping is not unison but soon everyone is clapping at the same frequency and phase with others. Most spectacular phenomenon is simultaneous flashing

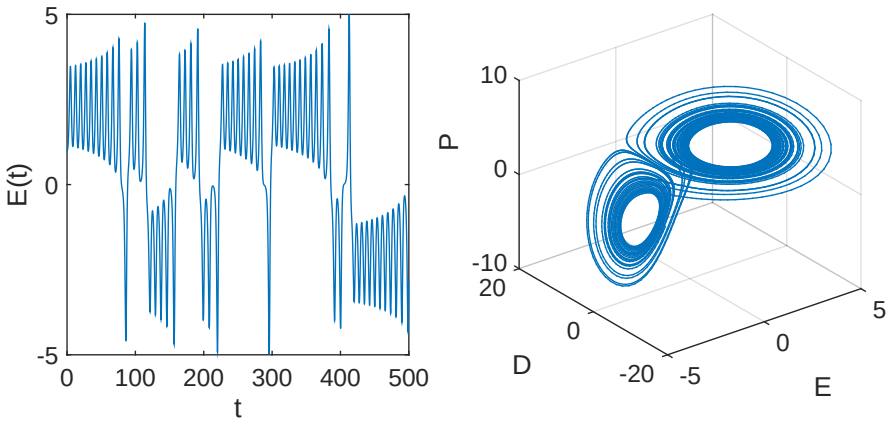

Figure 5.11: Left: Erroneous oscillation in the magnitude of electric field. Right: Three–dimensional phase plot of E, P and D showing a strange attractor. Parameter values: Type C in Table 5.1 and $\lambda = 23$

of thousands of fireflies in Southeast Asia.[7, 8] An example in physics is synchronization of the array of Josephson junctions.[7]

We investigate a similar phenomena using the Kuramoto model. The dynamics of phase variables θ_1 and θ_2 is described by a coupled ODEs[9]:

$$\dot{\theta_1} = \omega_1 + \sin(\theta_2 - \theta_1) \tag{5.40a}$$
$$\dot{\theta_2} = \omega_2 - \sin(\theta_2 - \theta_1) \tag{5.40b}$$

where ω_1 and ω_2 are natural frequencies of the individual phase oscillator. When there is no coupling, each oscillator oscillates with its own frequency. This problem is similar to the two car problem (Example 5.4). However, the coupling is now nonlinear and more dramatic phenomena such as phase entrainment and synchronization can be seen in this model. Program 5.9 integrates Eq. (5.40) with the 2nd-order Runge-Kutta method. The results are plotted in Fig. 5.12. Initially the oscillators are in different phases and periods. Despite of their different natural frequencies, they oscillates in the exactly the same period (frequency entrainment) and with a constant phase difference (phase synchronization).

Exercise 5.3 Observe that for $\omega_1 = 1.0$ and $\omega_2 = 2.2$, frequency entrainment still takes place. However, the phase difference no longer vanishes.

Exercise 5.4 Observe that for $\omega_1 = 1.0$ and $\omega_2 = 3.2$, neither frequency entrainment nor phase synchronization occur. The difference between the two oscillators is too big,

5.5.4 Period of Oscillation

In Sec 3.6.1, we discussed how to evaluate the analytical expression of the period of oscillation using numerical integration. Here we simulate the oscillation by solving the Newton's equation of motion numerically. We assume that the analytical form of the force, $F(x) = -U'(x)$, is known. You can pick any initial condition consistent with the given energy E. For example, the initial position x_0 is chosen somewhere between two turning points. The initial velocity is then determined by the energy conservation law

$$\frac{m}{2}v_0^2 + U(x_0) = E \quad \rightarrow \quad v_0 = \pm\sqrt{\frac{2(E - U(x_0))}{m}} \tag{5.41}$$

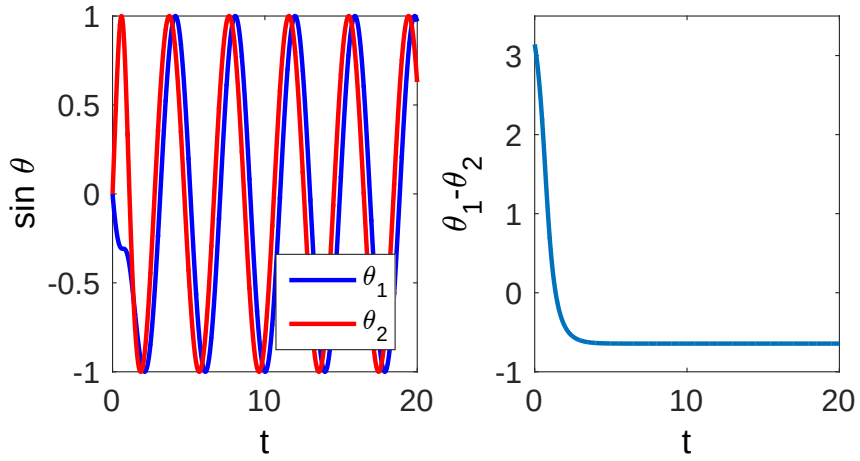

Figure 5.12: Left: The trajectory of the oscillators. Each oscillator has its own natural frequency $\omega_1 = 1.0$ and $\omega_2 = 1.2$. Initially the two oscillators are out of phase. Despite of these differences, they are quickly synchronized and oscillate at the same frequency. Left: the phase difference rapidly changes at the beginning but settles to a constant phase difference. [The 2nd-order Runge-Kutta is used with $h = 0.01$.]

The sign determines the direction of initial velocity.

To determine the period of oscillation, we measure the time the particle comes back to the starting point. To increase accuracy, we measure the time τ the particle returns to the starting point after N oscillations. Then, the period is $T = \tau/N$. One problem is that the time is discrete and we don't know the exact time the particle returned. Suppose that the particle passes the initial position between t_n and t_{n+1}. That means $t_n < \tau < t_{n+1}$ and $x_n < x_0 < x_{n+1}$ (assuming that the direction of the initial velocity is positive.) Using the Euler method, the time to reach the starting point is $\tau = t_n + \delta$ where $delat$ is a positive solution of quadratic equation

$$x_0 = x_n + v_n\delta + F_n\frac{\delta^2}{2m} \tag{5.42}$$

for $\delta = t_{n+1} - \tau$. Choosing the smaller root, the answer is

$$\delta = \frac{-v_n \pm \sqrt{v_n^2 - 2(x_n - x_0)F_n/m}}{F_n/m} \tag{5.43}$$

One of the solutions are positive depending on the sign of the force F_n. Since $x_n - x_0$ may be very small, we need to take care of the bit-off error discussed in Problem 1.1. Program 5.11 evaluates the period of simple harmonic oscillator (see Example 5.5) using the Verlet method. With $h = 0.05$, the Verlet method predicts $T = 6.283159$, in a good agreement with the exact answer $T = 2\pi$.

5.5.5 Pendulum

A pendulum consisting of a bob of mass m and a massless rod of length ℓ exhibits two types of motion, oscillation around a stable equilibrium and rotation in one way. Using the angular coordinate, the equation of motion of a simple pendulum is

$$I\ddot{\theta} = -mg\ell\sin\theta \tag{5.44}$$

where $I = m\ell^2$ is the moment of inertia. Simplifying the equation,

$$\ddot{\theta} = -\Omega^2\sin\theta \tag{5.45}$$